Biomaterials 33 (2012) 7233–7240

Contents lists available at SciVerse ScienceDirect

Biomaterials

journal homepage: www.elsevier.com/locate/biomaterials

Cellular uptake and intracellular trafficking of PEG-*b*-PLA polymeric micelles

Zhen Zhang [a,b,1], Xiaoqin Xiong [a,1], Jiangling Wan [a,1], Ling Xiao [a], Lu Gan [a,*], Youmei Feng [b], Huibi Xu [a], Xiangliang Yang [a,*]

[a] National Engineering Research Center for Nanomedicine, College of Life Science and Technology, Huazhong University of Science and Technology, Wuhan 430074, China
[b] Department of Biochemistry and Molecular Biology, Tongji Medical College, Huazhong University of Science and Technology, Wuhan 430030, China

ARTICLE INFO

Article history:
Received 11 May 2012
Accepted 22 June 2012
Available online 15 July 2012

Keywords:
Polymeric micelles
Cellular uptake
Intracellular trafficking
Nile red

ABSTRACT

Besides as an inert carrier for hydrophobic anticancer agents, polymeric micelles composed of di-block copolymer poly(ethylene glycol)–poly(lactic acid) (PEG-*b*-PLA) function as biological response modifiers including reversal of multidrug resistance in cancer. However, the uptake mechanisms and the subsequent intracellular trafficking remain to be elucidated. In this paper, we found that the uptake of PEG-*b*-PLA polymeric micelles incorporating nile red (M-NR) was significantly inhibited by both dynamin inhibitor dynasore and dynamin-2 dominant negative mutant (dynamin-2 K44A). Exogenously expressed caveolin-1 colocalized with M-NR and upregulated M-NR internalization in HepG2 cells expressing low level of endogenous caveolin-1, while caveolin-1 dominant negative mutant (caveolin-1 Y14F) significantly downregulated M-NR internalization in C6 cells expressing high level of endogenous caveolin-1. Exogenously expressed clathrin light chain A (clathrin LCa) did not mainly colocalize with the internalized M-NR and had no effect on M-NR uptake. These results suggested that dynamin- and caveolin-dependent but clathrin-independent endocytosis was involved in M-NR cellular uptake. We further found that M-NR colocalized with lysosome and microtubulin after internalization.

1. Introduction

The understanding of the cellular uptake mechanisms and intracellular trafficking remains a major challenge for developing effective nano drug delivery systems (NDDS) [1]. Among various NDDS, polymeric micelles with nano-sized core–shell structure have received growing attention in recent years owing to their good biocompatibility, long circulation, capability to solubilize hydrophobic drugs and selective tumor targeting [2,3]. Currently, five polymeric micelles-based anticancer drugs including Genexol-PM, NK911, NK105, NC-6004 and NK012 have been under clinical trials, of which Genexol-PM has been FDA approved for use in patients with breast cancer [4–8]. However the mechanisms governing the cellular uptake of polymeric micelles-based drug delivery systems and their intracellular fate are not well understood.

Polymeric micelles not only function as inert carriers for hydrophobic anticancer agents such as paclitaxel (PTX) and doxorubicin (DOX) but also as biological response modifiers [9]. Our previous work showed that polymeric micelles composed of di-block copolymer poly(ethylene glycol)–poly(lactic acid) (PEG-*b*-PLA), an FDA approved pharmaceutical excipient, can inhibit P-glycoprotein (Pgp) function to reverse multidrug resistance (MDR) in cancer. Further studies on its relevance of cellular uptake and reversal of MDR showed that the inhibition of Pgp function by PEG-*b*-PLA micelles might be related to their interaction with the cell membrane and subsequent lipid raft-mediated endocytosis, considering that the uptake was inhibited by cholesterol-depleting reagent methyl-β-cyclodextrin (MβCD) but not by clathrin-dependent endocytosis inhibitor chlorpromazine [10]. Although the use of chemical inhibitors is quite common, they often lead to nonspecific disruption in the cell [11]. For this reason, the detailed uptake and intracellular trafficking mechanisms by PEG-*b*-PLA micelles remain to be explored. In this paper we used plasmids encoding wild type or dominant negative forms of proteins in the endocytic pathway, which provide a more specific way to analyze the function of defined pathways [12], to elucidate the uptake mechanism. The subsequent intracellular trafficking was further assessed by colocalization with specific cell compartments using confocal microscopy.

2. Materials and methods

2.1. Materials

PEG-PLA di-block polymer (PEG(5000)-*b*-PLA(5000)) was purchased from Daigang Biotechnology Co. Ltd (Jinan, China). Nile red (NR), Trizol, SuperScript II reverse transcriptase and LysoTracker Green were purchased from Molecular Probes/

* Corresponding authors. Tel.: +86 27 8779 4520; fax: +86 27 8779 4517.
E-mail addresses: lugan@mail.hust.edu.cn, ganlu_74@hotmail.com (L. Gan), yangxl@mail.hust.edu.cn (X. Yang).
[1] These authors contributed equally to this work.

0142-9612/$ – see front matter © 2012 Elsevier Ltd. All rights reserved.
http://dx.doi.org/10.1016/j.biomaterials.2012.06.045

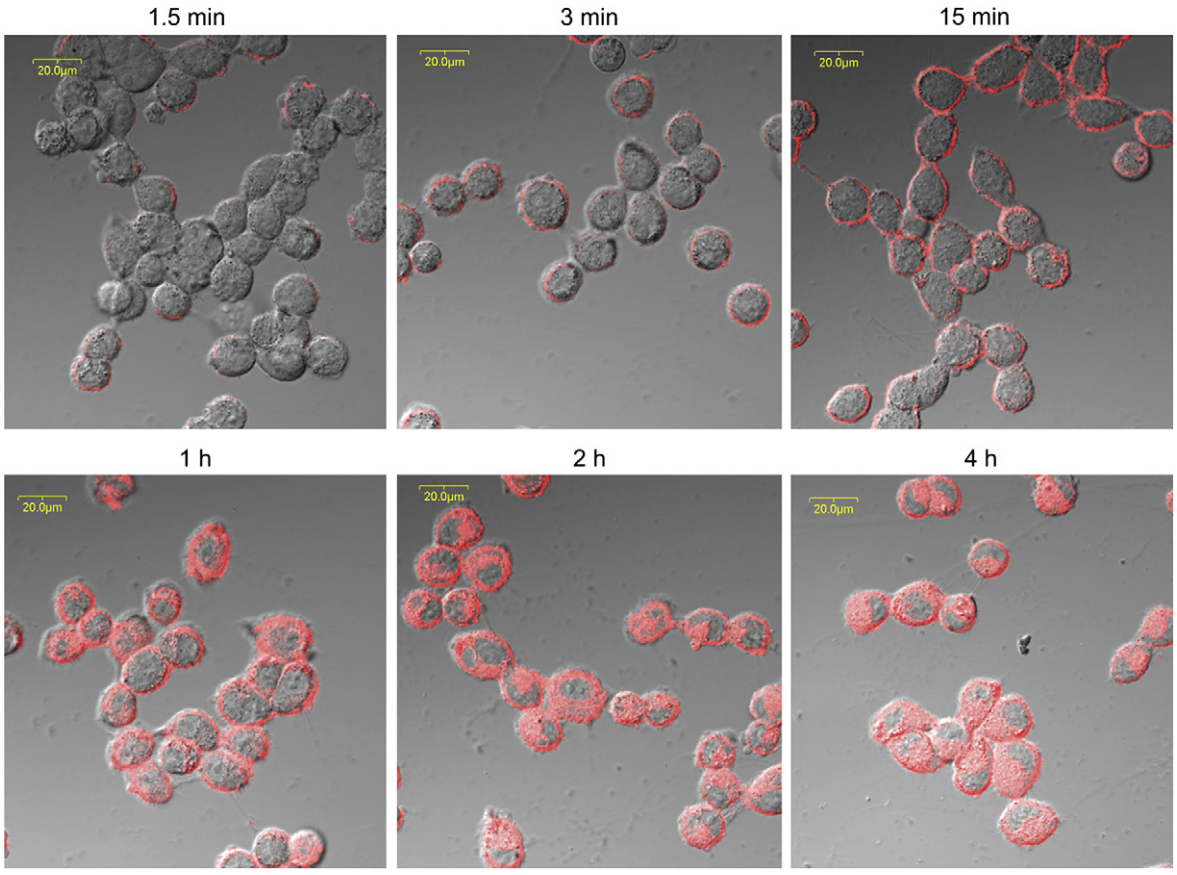

Fig. 1. Confocal microscopy images of the uptake process of M-NR in A2780 cells after treatment with 0.2 mg/ml M-NR for 1.5 min, 3 min, 15 min, 1 h, 2 h and 4 h, respectively. The red and bright fields were overlaid. (For interpretation of color in this figure legend, the reader is referred to web version of the article.)

Invitrogen (Carlsbad, CA, USA). Dynasore was purchased from Sigma–Aldrich (St Louis, MO, USA). DiO was obtained from Beyotime Institute of Biotechnology (Jiangsu, China). Dulbecco's modified Eagle medium (DMEM), RPMI 1640 medium and fetal bovine serum (FBS) were purchased from Gibco BRL/Life Technologies (Grand Island, NY, USA). All other chemicals used were of analytical grade commercially available.

2.2. Cell culture

The human hepatocellular carcinoma cell line HepG2 and human cervical carcinoma cell line HeLa were purchased from China Center for Type Culture Collection (Wuhan, China). The human ovarian A2780 cells and rat C6 glioma cells were kindly provided by Profs. Ding Ma and Haibo Xu (Huazhong University of

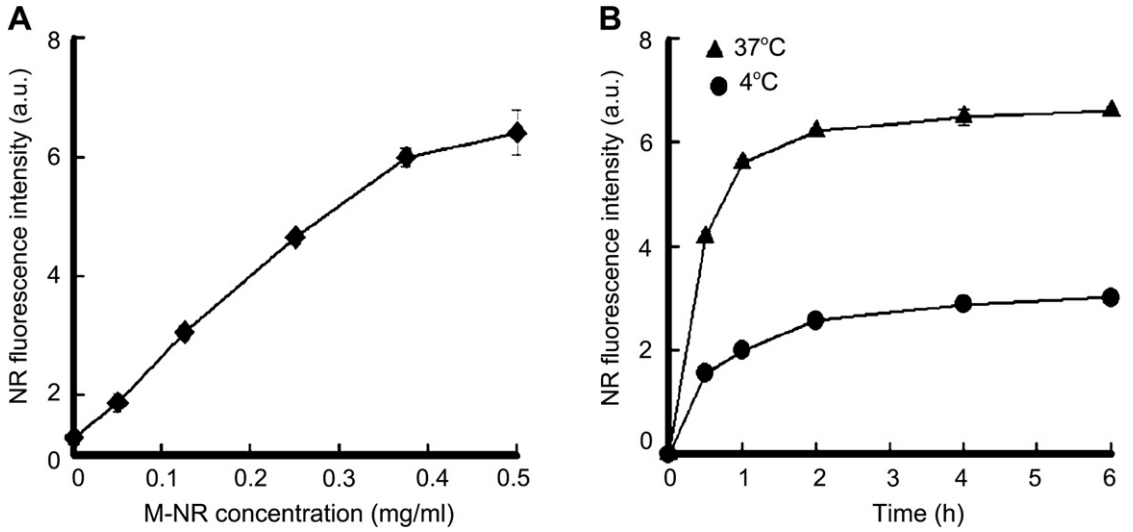

Fig. 2. The concentration-, incubation time- and energy-dependent curves of the cellular internalization of M-NR. (A) The internalization curves in A2780 cells after treatment with 0.05, 0.125, 0.25, 0.375, 0.5 mg/ml M-NR for 4 h at 37 °C. (B) The internalization curves in A2780 cells after treatment with 0.5 mg/ml M-NR for 0.5, 1, 2, 4, 6 h at 4 °C and 37 °C, respectively. Data as mean values ± S.D. ($n = 3$).

Science and Technology, Wuhan, China) respectively. C6 cells were cultured in DMEM medium and A2780, HepG2 and HeLa cells were cultured in RPMI 1640 medium at 37 °C in 5% CO_2 in a humidified atmosphere. All media contained 10% FBS, 100 U/ml penicillin and 100 μg/ml streptomycin.

2.3. Preparation of polymeric micelles

NR-loaded PEG-*b*-PLA polymeric micelles (M-NR) were prepared by thin film method [13]. Briefly, 0.05 mg NR and 50 mg PEG-*b*-PLA were dissolved in 2 ml acetonitrile in a round-bottom flask. The solvent was evaporated by rotary evaporation at 60 °C for about 1 h to obtain a solid NR/copolymer matrix. Residual acetonitrile remaining in the film was removed under vacuum overnight at room temperature. The resultant thin film was hydrated with 10 ml water at 60 °C for 30 min to obtain a micelle solution, which was then filtrated through a 0.22 μm Millipore filter membrane to remove the unincorporated NR aggregates.

2.4. Plasmid amplification

Plasmids expressing green fluorescent proteins (GFPs) fused to dynamin-2 (GFP-dynamin-2), clathrin light chain A (GFP-clathrin LCa) and caveolin-1 (GFP-caveolin-1) were kindly provided by Dr. Rongying Zhang (Huazhong University of Science and Technology, Wuhan, China). Plasmids expressing GFPs fused to endoplasmic reticulum (GFP-ER) and tubulin (GFP-tubulin) were kindly provided by Dr. Ting Peng (Huazhong University of Science and Technology, Wuhan, China). Plasmids expressing GFP-dynamin-2 K44A and GFP-caveolin-1 Y14F were generated by PCR-based mutagenesis according to the manufacturer's instruction (Stratagene, La Jolla, CA, USA). To amplify these plasmids, plasmids were proliferated firstly in *Escherichia coli* DH5α strain and then purified using QIAGEN plasmid purification kits (QIAGEN Sciences Inc, Germantown, MD, USA) following the manufacturer's instruction. The plasmids obtained were identified by restriction enzymes and sequencing. The concentration and purity of plasmid preparations were determined by UV spectrophotometry.

2.5. Gene transfection

Transfections by electroporation were performed as described [14]. Briefly, the cells were trypsinized and 1×10^7 cells were resuspended in 350 μl serum-free RPMI 1640 medium. Ten microgram of plasmid DNA was diluted in 50 μl serum-free RPMI 1640 medium and then added into the resuspended cells. The mixtures of cells and DNA were kept at room temperature for 5 min and then transferred into a 4-mm cuvette. The electroporation was carried out using Gene Pulser II Electroporation System (Bio-Rad, Richmond, CA, USA). The electroporated cells were replated into 3 wells in the 6-well plates and cultured with DMEM or RPMI 1640 medium containing 10% FBS for 24 h. Approximately 75–90% transfection efficiencies were routinely achieved.

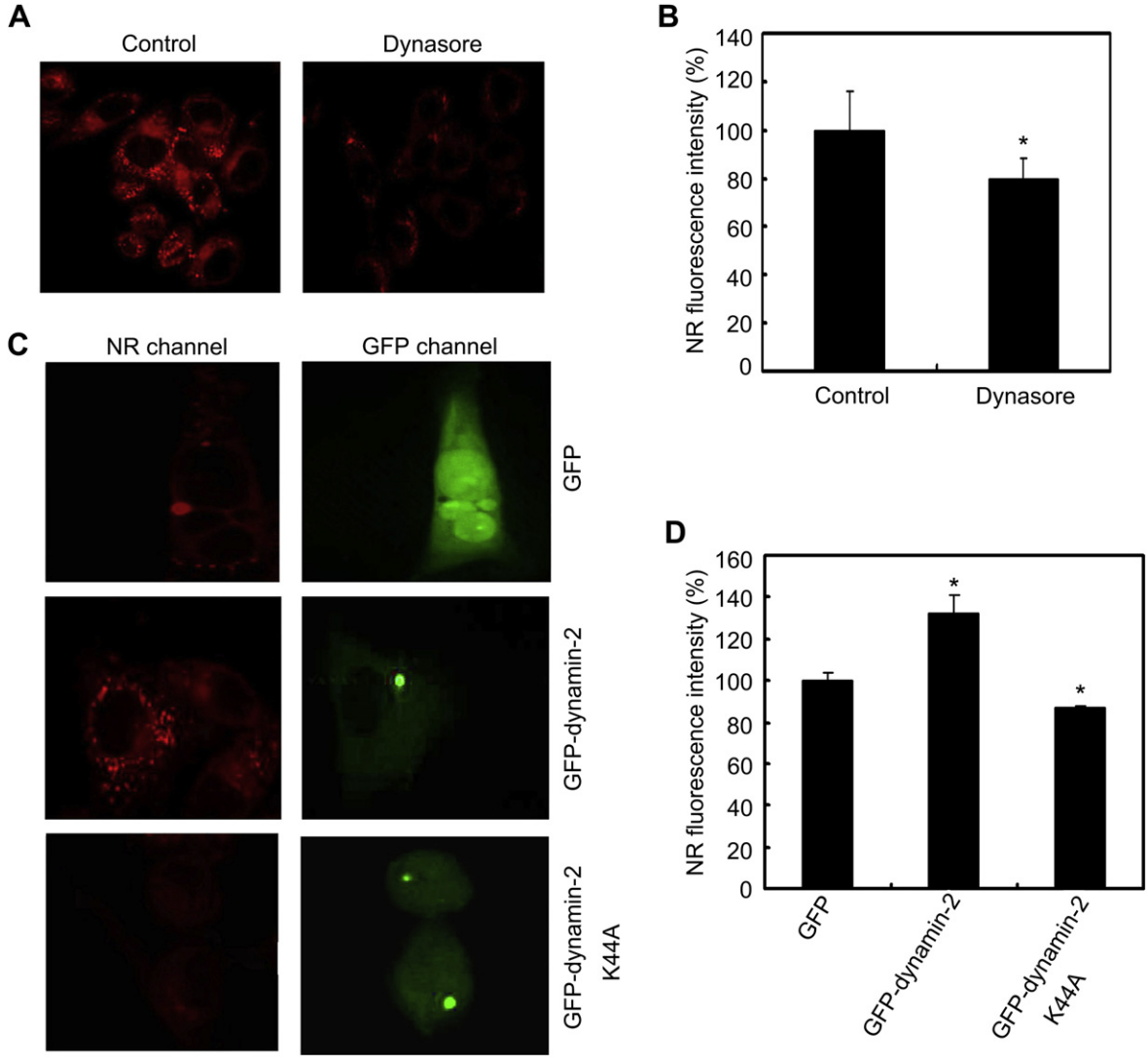

Fig. 3. Dynamin-dependent endocytosis of M-NR. (A) Confocal microscopy images of M-NR uptake when A2780 cells were pretreated with or without 80 μM dynarose for 1 h and then treated with 0.2 mg/ml M-NR for 1 h. (B) Percentages of the internalized NR fluorescence intensity when A2780 cells were pretreated with or without 80 μM dynarose for 1 h and then treated with 0.2 mg/ml M-NR for 1 h by flow cytometry. Data as mean values ± S.D. ($n = 3$). *$P < 0.05$ compared with control group. (C) Confocal microscopy images of M-NR internalization in A2780 cells expressing GFP, GFP-dynamin-2 or GFP-dynamin-2 K44A after treated with 0.2 mg/ml M-NR for 1 h. (D) Percentages of the internalized NR fluorescence intensity in A2780 cells expressing GFP, GFP-dynamin-2 or GFP-dynamin-2 K44A after treated with 0.2 mg/ml M-NR for 1 h by flow cytometry. Data as mean values ± S.D. ($n = 3$). *$P < 0.05$ compared with control group expressing GFP.

2.6. Reverse transcription-polymerase chain reaction (RT-PCR)

Total cellular RNAs were isolated from the cells using Trizol and complementary DNAs (cDNAs) were synthesized using SuperScript II reverse transcriptase according to the manufacturer's instruction. The cDNAs were amplified in a PCR reaction using primers specific for caveolin-1 (forward 5′-ATCTACAAGCCCAACAAC-3′ and reverse 5′-TCTCAATCAGGAAGCTCT-3′), and glyceraldehyde-3-phosphate dehydrogenase (GAPDH, forward 5′-ACCCACTCCTCCACCTTTGA-3′ and reverse 5′-CTGTTGCTGTAGCCAAATTCGT-3′). After heating samples at 94 °C for 5 min, 35 cycles of PCR were performed consisting of denaturation at 94 °C for 1 min, annealing at 55 °C for 45 s, and extension at 72 °C for 1 min with a final extension at 72 °C for 10 min. The PCR products were separated on a 2% agarose gel containing ethidium bromide (0.5 μg/ml).

2.7. The cellular uptake of M-NR

Cells were seeded in 24-well plates at a density of 3×10^4 cells per well for 24 h. Cells were washed with phosphate buffered saline (PBS) and then treated with different concentrations of M-NR for different time courses as described in figure legends. To observe the uptake process of M-NR, the treated cells were washed three times with PBS and then imaged using Olympus FV 500 confocal microscope (Olympus, Tokyo, Japan). Flow cytometry and fluorescence spectrophotometery were carried out to quantify the internalized M-NR.

For flow cytometric analysis, the treated cells were washed with PBS, trypsinized and then harvested by centrifugation at 1000 rpm for 5 min. The cells were resuspended in 500 μl PBS and filtered through a 40 μm nylon mesh to remove cell aggregates. The cell suspensions were then analyzed by flow cytometry (FC500, Beckman Coulter, USA).

For fluorescence spectrophotometric analysis, the treated cells were lysed in 800 μl of 0.1% Triton X-100 after washing with PBS and then centrifuged at 12,000 rpm for 5 min. The fluorescence intensity of the supernatants was measured with the excitation wavelength at 546 nm and emission wavelength at 574 nm.

2.8. Endocytic pathway of M-NR

Cells were transfected with the plasmids expressing GFP, GFP-dynamin-2, GFP-dynamin-2 K44A, GFP-caveolin-1, GFP-caveolin-1 Y14F and GFP-clathrin LCa, respectively. After 24 h transfection, the cells were treated with 0.2 mg/ml M-NR for 1 h. For qualitative analysis of the effects of endocytic proteins on the uptake of M-NR, the treated cells were washed with PBS and then imaged using an Andor Revolution spinnig disk confocal microscope (Andor Technology, Germany). Images of GFP and NR fluorescence were obtained using standard filter sets (excitation at 491 nm, emission at 495–550 nm for GFP; excitation at 561 nm, emission at 566–611 nm for NR) and merged afterwards. For quantitative analysis, the treated cells were washed and subjected to flow cytometry for expression of both GFP and NR.

2.9. Intracellular localization of M-NR

For assessment of colocalization of M-NR with ER or microtubule, A2780 cells were transfected with GFP-ER or GFP-tubulin. After 24 h transfection, the cells were treated with 0.2 mg/ml M-NR for 1 h, washed with PBS and then fixed in 4% paraformaldehyde for 15 min at room temperature. For assessment of colocalization of M-NR with lysosome or plasma membrane, A2780 cells were treated with 0.2 mg/ml M-NR for 1 h, washed with PBS and then incubated with medium containing 100 nM Lysotracker Green (a lysosomal marker) or 10 μM DiO (a plasma membrane marker) at 37 °C for 30 min before fixation. The cells were observed under an Andor Revolution spinning disk confocal microscope. Images of GFP and NR fluorescence were obtained using standard filter sets and merged afterwards.

2.10. Statistical analysis

Experiments were carried out with three or four replicates. Statistical analyses were performed by Student's *t* test. Values with $P < 0.05$ are considered significant.

3. Results and discussion

3.1. The cellular uptake process of M-NR

NR as a model drug was incorporated into PEG-*b*-PLA micelles by thin film method with an average diameter of 44.7 nm and the critical micelle concentration of 1.5 μg/ml [10]. To determine the interaction of PEG-*b*-PLA micelles with the cells, we firstly observed the uptake process of M-NR in human ovarian cell line A2780 by confocal microscope. As shown in Fig. 1, the cell membrane was slightly luminescent after 1.5 min incubation with M-NR. The fluorescence intensity increased in the cell membrane but was almost undetectable in cytoplasm at 15 min. After 1 h incubation, cells showed remarkable fluorescence in the cytoplasm. As time went on (2 h and 4 h), the intracellular fluorescence intensity gradually increased.

3.2. Concentration, incubation time and energy-dependent uptake of M-NR

To further determine the rule of M-NR uptake in the cells, A2780 cells were treated with different concentrations of M-NR for different time courses. As shown in Fig. 2, an increase in M-NR concentration and incubation time resulted in the increased M-NR uptake. To determine whether the energy-dependent endocytosis was involved in the uptake, A2780 cells were treated with M-NR at 37 °C or 4 °C as endocytosis can be inhibited by lowering the temperature [15]. We found that M-NR uptake was greatly decreased at 4 °C. These data indicated that a concentration, incubation time and energy-dependent endocytosis was involved in the uptake of M-NR.

3.3. Effects of dynamin on the uptake of M-NR

Dynamin GTPase has been widely characterized to involve in many pathways of endocytosis, including clathrin, caveolin or macropinocytosis [16–18]. Dynamin self-assembles into a helical structure to wrap around the necks of newly formed budded

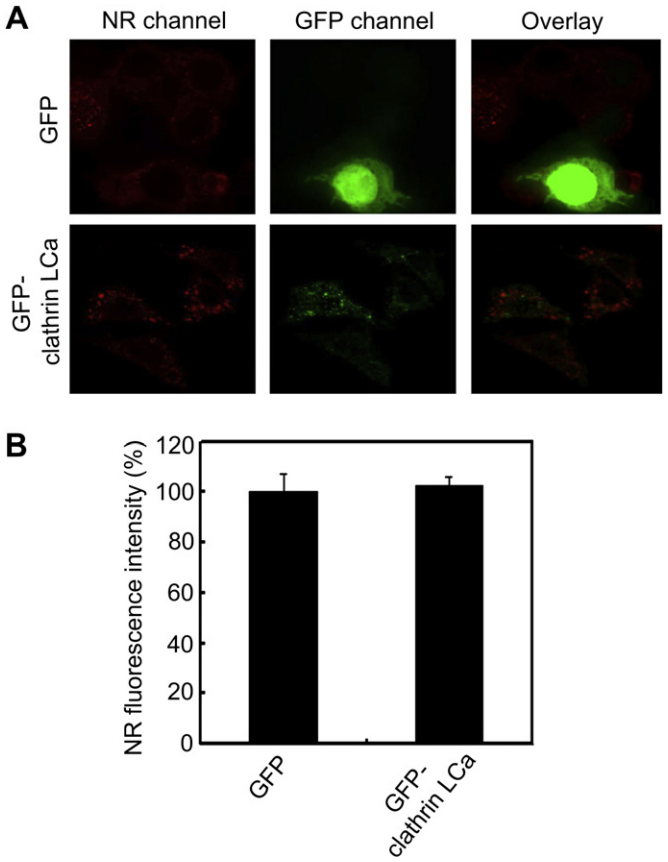

Fig. 4. Clathrin-independent endocytosis of M-NR. (A) Confocal microscopy images of M-NR internalization in A2780 cells expressing GFP or GFP-clathrin LCa after treated with 0.2 mg/ml M-NR for 1 h. (B) Percentages of the internalized NR fluorescence intensity in A2780 cells expressing GFP or GFP-clathrin LCa after treated with 0.2 mg/ml M-NR for 1 h by flow cytometry. Data as mean values ± S.D. ($n = 3$).

vesicles and then pinches them off from the cell plasma membrane, freeing them into the cytoplasma [19,20]. Without functional dynamin, some endocytic vesicles such as caveolin or clathrin-coated vesicles cannot be formed to transport their cargo from plasma membrane to various other destinations in the cell. To test whether dynamin was involved in the cellular uptake of M-NR, A2780 cells were pretreated with dynasore [21], a small cell-permeable molecule that inhibits dynamin GTPase for 1 h and then exposed to M-NR. As shown in Fig. 3A, dynasore significantly reduced M-NR uptake by confocal microscopy. The quantitative results obtained from flow cytometry (Fig. 3B) were consistent with the qualitative results from confocal microscopy studies, suggesting that M-NR uptake might be dynamin-dependent. To further confirm dynamin was involved in M-NR uptake, A2780 cells were transfected with GFP-fused wild type dynamin-2 or its dominant negative mutant dynamin-2 K44A which is unable to hydrolyze GTP [22]. Successful transfection of A2780 cells was verified by detection of GFP expression (GFP channel in Fig. 3C). Confocal microscopy and flow cytometric analysis showed that over-expression of wild type dynamin-2 significantly increased M-NR internalization compared with empty vector, while specific inhibition of dynamin-2 GTPase function by overexpression of dynamin-2 K44A significantly inhibited M-NR internalization (Fig. 3C and D). The effects of wild type dynamin-2 and dynamin-2 K44A on the M-NR uptake in C6 cells are similar to those in A2780 cells (data not shown). These data indicated that dynamin was involved in the uptake of PEG-*b*-PLA micelles.

3.4. Role of clathrin in the uptake of M-NR

Based on our results showing the requirement for dynamin-2 in the M-NR uptake, the question remained which endocytic pathway was dominating M-NR uptake. Clathrin-mediated endocytosis is one of the most well-characterized uptake mechanism [23]. In our previous work [10], pretreatment with chlorpromazine, an inhibitor to probe clathrin-mediated endocytosis, did not affect the M-NR uptake, suggesting that clathrin-independent endocytosis was involved in M-NR uptake. To further test the role of clathrin, A2780 cells were transfected with clathrin light chain A fused to GFP (GFP-clathrin LCa) and then treated with M-NR. As shown in Fig. 4A, most of the internalized M-NR (NR channel) did not colocalize with GFP-clathrin LCa (GFP channel). Furthermore, clathrin LCa did not affect the M-NR uptake by confocal microscopy and flow cytometry (Fig. 4A and B). Recently Sahay et al. reported that Pluronic P85 unimers internalized through caveolae-mediated endocytosis below the critical micelle concentration, while Pluronic P85 micelles internalized through clathrin-mediated endocytosis above the critical micelle concentration [24]. In our work the concentration of PEG-*b*-PLA micelles was 0.2 mg/ml, which was much higher than the critical micelle concentration to ensure the integrity of micelles. The difference of endocytic pathway between PEG-*b*-PLA micelles and pluronic P85 micelles might be due to the different materials and the different properties of the nanoparticles.

3.5. Role of caveolin in the uptake of M-NR

To investigate the mechanisms of M-NR endocytosis, we examined a possible role for caveolin in M-NR internalization considering that M-NR uptake was inhibited by MβCD [10]. Firstly, the internalization of M-NR was determined in three cell lines containing a variety of caveolin-1 expression as illustrated by RT-PCR. Consistent with published reports [25], C6 cells had the most endogenous caveolin-1 expression whereas very low levels of caveolin-1 were detected in HepG2 and HeLa cells (Fig. S1).

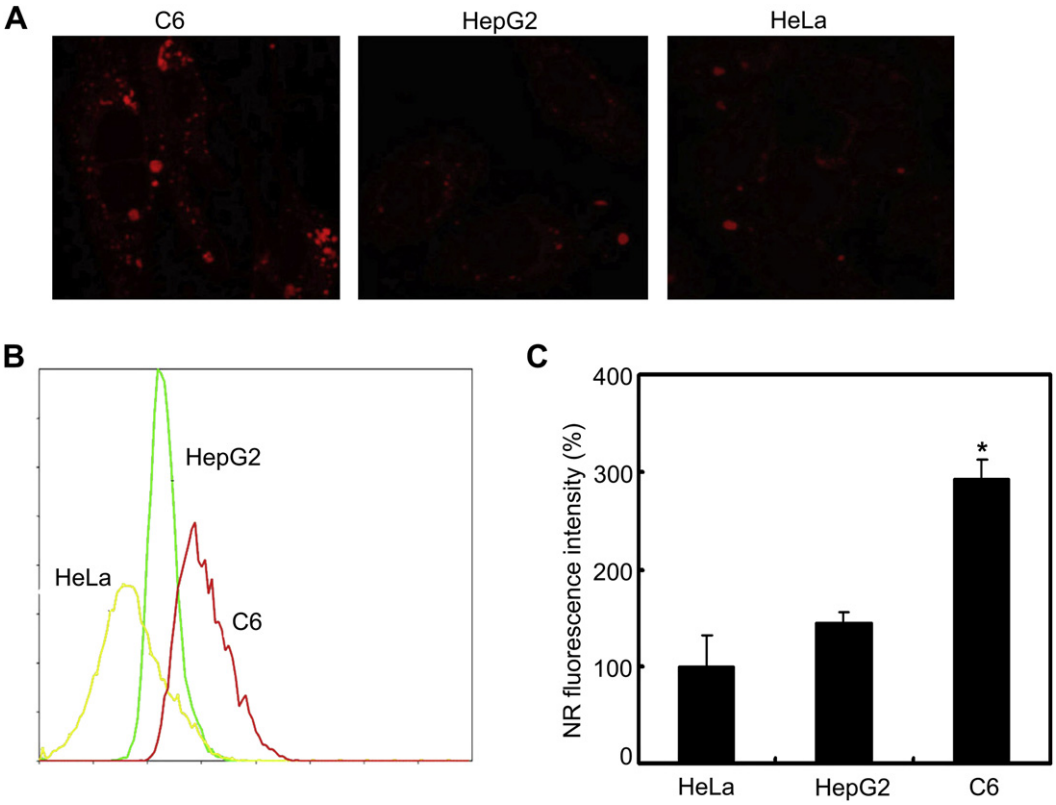

Fig. 5. The internalization of M-NR in cells expressing different levels of caveolin-1. (A) Confocal microscopy images of M-NR internalization in C6, HepG2 and HeLa cells after treated with 0.2 mg/ml M-NR for 1 h. (B) The flow cytometric results of M-NR internalization in C6, HepG2 and HeLa cells after treated with 0.2 mg/ml M-NR for 1 h. (C) Percentages of the internalized NR fluorescence intensity in C6, HepG2 and HeLa cells quantified from (B). Data as mean values ± S.D. ($n = 3$). *$P < 0.01$ compared with the group in HeLa cells.

Correspondingly, we found that the fluorescence intensity of the internalized M-NR was the most in C6 cells by flow cytometry and confocal microscopy (Fig. 5A, B and C), suggesting that caveolin-1 might be involved in the uptake of PEG-*b*-PLA polymeric micelles.

To further confirm that caveolin-1 was involved in the endocytic pathway of PEG-*b*-PLA polymeric micelles, C6 cells and HepG2 cells were transfected with GFP- tagged wild type caveolin-1 and its dominant negative mutant caveolin-1 Y14F, which has been reported to disrupt caveolae and prevent caveolin-mediated endocytosis [26]. As shown in Fig. 6A and C, caveolin-1 (GFP channel), an established marker of caveolin-dependent endocytosis, colocalized with M-NR (NR channel) using confocal microscopy. Compared with GFP empty vector, wild type caveolin-1 significantly increased the fluorescence intensity of internalized M-NR in HepG2 cells expressing low level of caveolin-1 (Fig. 6A), while dominant negative mutant caveolin-1 Y14F significantly decreased the fluorescence intensity of internalized M-NR in C6 cells expressing high level of caveolin-1 (Fig. 6C). The effects of wild type

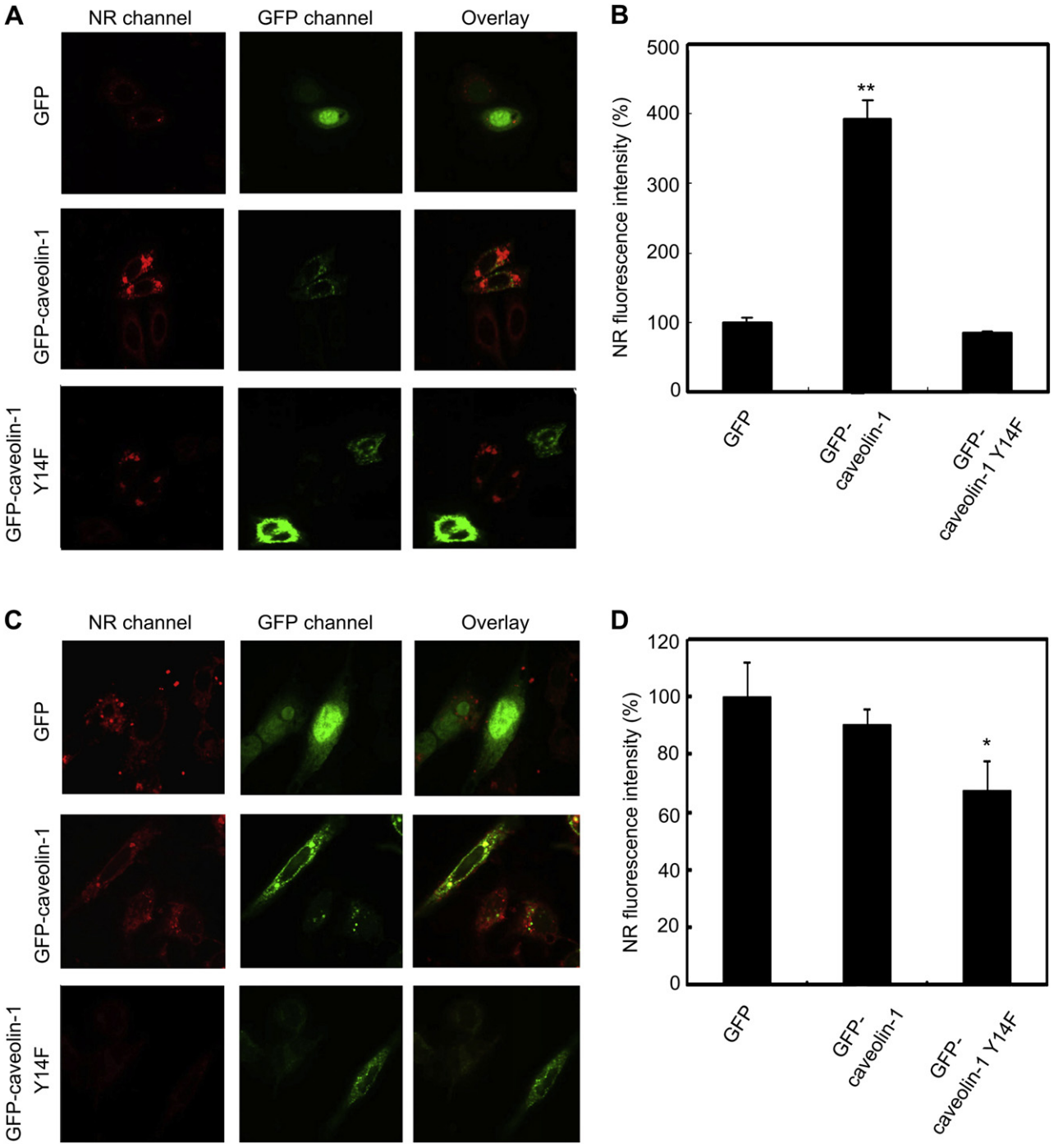

Fig. 6. Caveolin-dependent endocytosis of M-NR uptake. (A, C) Confocal microscopy images of M-NR internalization in HepG2 cells (A) and C6 cells (C) expressing GFP, GFP-caveolin-1 or GFP-caveolin-1 Y14F after treated with 0.2 mg/ml M-NR for 1 h. (B, D) Percentages of the internalized NR fluorescence intensity in HepG2 cells (B) and C6 cells (D) expressing GFP, GFP-caveolin-1 or GFP-caveolin-1 Y14F after treated with 0.2 mg/ml M-NR for 1 h by flow cytomentry. Data as mean values ± S.D. ($n = 3$). *$P < 0.05$ compared with control group expressing GFP.

caveolin-1 and caveolin-1 Y14F mutant on the cellular uptake in HepG2 and C6 cells were further confirmed by flow cytometry (Fig. 6B and D). However we found that the introduction of wild type caveolin-1 in C6 cells and caveolin-1 Y14F in HepG2 cells did not affect M-NR uptake, that's perhaps because the initial caveolin-1 expressions were abundant in C6 cells while rare in HepG2 cells.

It is noteworthy that none of the dominant negative mutants of either caveolin-1 or dynamin-2 alone completely inhibited M-NR internalization. One reason might be that these dominant negative mutants did not completely inhibit caveolin-1 function or dynamin GTPase. Another reason is that we could not rule out that other internalization mechanisms independent of these pathways might be involved in M-NR uptake. More detailed endocytic mechanisms involved remain to be further elucidated.

3.6. Intracellular trafficking of M-NR

It was reported that internalized nanoparticles by clathrin-dependent endocytosis were genereally entrapped in endosomes and then fused with lysosomes, resulting in lysosomal degradation of the cargo [27]. In comparison, the internalized nanoparticles by caveolin-mediated endocytosis usually could bypass lysosomal degradation and be directly transported to Golgi and/or ER [28]. However, some papers showed that the internalized caveolae also fused with endosomes and followed the classical endocytotic degradative pathway [29]. To track intracellular fate of M-NR following their uptake, confocal microscopy was used to demonstrate the colocalization of M-NR with cell compartments. As shown in Fig. 7, M-NR did not colocalize with cell membrane marker DiO and entered the cytoplasma after 4 h incubation. Most of internalized M-NR was localized in lysosome and only a small amount was detected to colocalize with ER, suggesting that the internalized PEG-*b*-PLA micelles were mainly delivered to lysosome and then the cargo might be released into the cytoplasma to take effect. We further found that M-NR colocalized with tubulin, a structural protein that builds the microtubule network of the cell. Considering that tubulin binds with dynamin and caveolin to affect caveolin expression and dyanmin GTPase [30,31], the colocalization of M-NR with tubulin might be helpful for dynamin- and caveolin-mediated endocytosis of M-NR uptake.

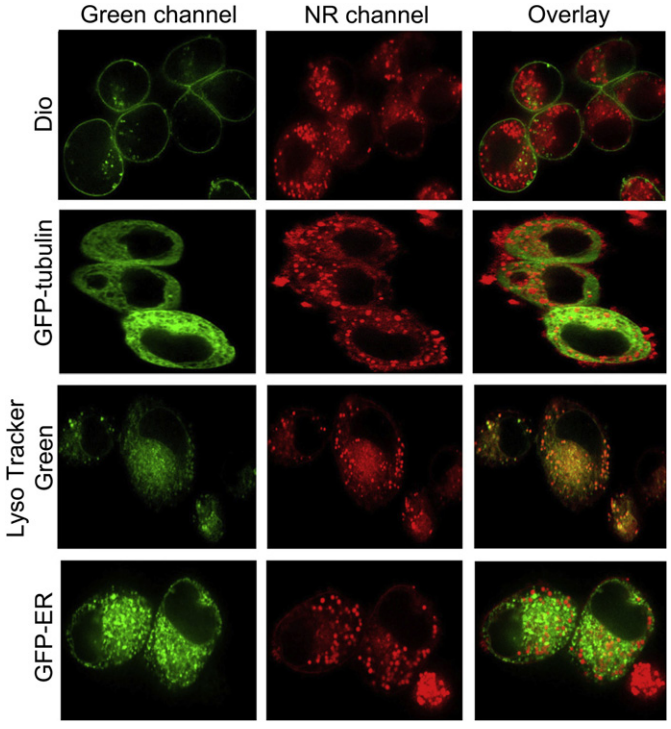

Fig. 7. Confocal microscopy images of the intracellular trafficking of M-NR after A2780 cells transfected with GFP-ER or GFP-tubulin were treated with 0.2 mg/ml M-NR for 1 h or A2780 cells were treated with 0.2 mg/ml M-NR for 1 h and then labeled with 10 μM DiO or 100 nM LysoTracker Green, respectively.

It was well known that the uptake mechanisms of nanoparticles into cells and their intracellular fates were influenced by the physiochemical properties of nanoparticles, such as surface charge, size and morphology [32]. To improve the therapeutic efficacy of PEG-*b*-PLA micelles as drug delivery system, the effects of physicochemical properties of PEG-*b*-PLA micelles on the cellular uptake mechanism and the intracellular trafficking needs to be further explored.

4. Conclusions

In summary, the endocytic pathway of PEG-*b*-PLA micelles and the subsequent intracellular trafficking were investigated. The results showed that dynamin- and caveolin-dependent but clathrin-independent endocytosis was involved in the uptake of PEG-*b*-PLA polymeric micelles. PEG-*b*-PLA micelles mainly colocalized with lysosome after internalization. The elucidation of the endocytosis and intracellular trafficking of PEG-*b*-PLA micelles is likely to provide a clue for understanding the diverse functions of this copolymer and developing more effective drug delivery systems.

Acknowledgement

We thank Profs. Ding Ma and Haibo Xu for the cells and Drs. Rongying Zhang and Ting Peng for the plasmids. We also thank the Analytical and Testing Center of Huazhong University of Science and Technology for related analysis. This work was supported by National Basic Research Program of China (973 Program, 2012CB932500 and 2011CB933100) and the National Natural Science Foundation of China (31070689).

Appendix A. Supplementary material

Supplementary data related to this article can be found online at http://dx.doi:10.1016/j.biomaterials.2012.06.045.

References

[1] Panyama J, Labhasetwara V. Biodegradable nanoparticles for drug and gene delivery to cells and tissue. Adv Drug Deliv Rev 2003;55:329–47.
[2] Nishiyama N, Kataoka K. Current state, achievements, and future prospects of polymeric micelles as nanocarriers for drug and gene delivery. Pharmacol Ther 2006;112:630–48.
[3] Sutton D, Nasongkla N, Blanco E, Gao J. Functionalized micellar systems for cancer targeted drug delivery. Pharm Res 2007;24:1029–46.
[4] Kim TY, Kim DW, Chung JY, Shin SG, Kim SC, Heo DS, et al. Phase I and pharmacokinetic study of genexol-PM, a cremophor-free, polymeric micelle-formulated paclitaxel, in patients with advanced malignancies. Clin Cancer Res 2004;10:3708–16.
[5] Matsumura Y. Poly (amino acid) micelle nanocarriers in preclinical and clinical studies. Adv Drug Deliv Rev 2008;60:899–914.
[6] Matsumura Y. Polymeric micellar delivery systems in oncology. Jpn J Clin Oncol 2008;38:793–802.
[7] Wang AZ, Langer R, Farokhzad OC. Nanoparticle delivery of cancer drugs. Annu Rev Med 2012;63:185–98.
[8] Oerlemans C, Bult W, Bos M, Storm G, Nijsen JFW, Hennink WE. Polymeric micelles in anticancer therapy: targeting, imaging and triggered release. Pharm Res 2010;27:2569–89.
[9] Kabanov AV, Batrakova EV, Miller DW. Pluronic block copolymers as modulators of drug efflux transporter activity in the blood-brain barrier. Adv Drug Deliv Rev 2003;55:151–64.
[10] Xiao L, Xiong X, Sun X, Zhu Y, Yang H, Chen H, et al. Role of cellular uptake in the reversal of multidrug resistance by PEG-*b*-PLA polymeric micelles. Biomaterials 2011;32:5148–57.

[11] Ivanov AI. Pharmacological inhibition of endocytic pathways: is it specific enough to be useful? Methods Mol Biol 2008;440:15–33.
[12] Sieczkarski SB, Whittaker GR. Dissecting virus entry via endocytosis. J Gen Virol 2002;83:1535–45.
[13] Gaucher G, Dufresne MH, Sant V, Kang N, Maysinger D, Leroux JC. Block copolymer micelles: preparation, characterization and application in drug delivery. J Control Release 2005;109:169–88.
[14] Gan L, Chen S, Wang Y, Watahiki A, Bohrer L, Sun Z, et al. Inhibition of the androgen receptor as a novel mechanism of taxol chemotherapy in prostate cancer. Cancer Res 2009;69:8386–94.
[15] Al-Jamal KT, Nerl H, Muller KH, Ali-Boucetta H, Li S, Haynes PD, et al. Cellular uptake mechanisms of functionalised multi-walled carbon nanotubes by 3D electron tomography imaging. Nanoscale 2011;3:2627–35.
[16] McLendon PM, Fichter KM, Reineke TM. Poly(glycoamidoamine) vehicles promote pDNA uptake through multiple routes and efficient gene expression via caveolae-mediated endocytosis. Mol Pharm 2010;7:738–50.
[17] Conner SD, Schmid SL. Regulated portals of entry into the cell. Nature 2003; 422:37–44.
[18] Nabi IR, Le PU. Caveolae/raft-dependent endocytosis. J Cell Biol 2003;161: 673–7.
[19] Mayor S, Pagano RE. Pathways of clathrin-independent endocytosis. Nat Rev Mol Cell Biol 2007;8:603–12.
[20] McNiven MA, Cao H, Pitts KR, Yoon Y. The dynamin family of mechanoenzymes: pinching in new places. Trends Biochem Sci 2000;25:115–20.
[21] Macia E, Ehrlich M, Massol R, Boucrot E, Brunner C, Kirchhausen T. Dynasore, a cell-permeable inhibitor of dynamin. Dev Cell 2006;10:839–50.
[22] Sweitzer SM, Hinshaw JE. Dynamin undergoes a GTP-dependent conformational change causing vesiculation. Cell 1998;93:1021–9.
[23] McMahon HT, Boucrot E. Molecular mechanism and physiological functions of clathrin-mediated endocytosis. Nat Rev Mol Cell Biol 2011;12:517–33.
[24] Sahay G, Batrakova EV, Kabanov AV. Different internalization pathways of polymeric micelles and unimers and their effects on vesicular transport. Bioconjug Chem 2008;19:2023–9.
[25] Manunta M, Nichols BJ, Tan PH, Sagoo P, Harper J, George AJT. Gene delivery by dendrimers operates via different pathways in different cells, but is enhanced by the presence of caveolin. J Immunol Methods 2006;314:134–46.
[26] Delva E, Jenning JM, Calkins CC, Kottke MD, Faundez V, Kowalczyk AP. Pemphigus vulgaris IgG-induced desmoglein-3 endocytosis and desmosomal disassembly are mediated by a clathrin and dynamin-independent mechanism. J Biol Chem 2008;283:18303–13.
[27] Khalil I, Kogure K, Akita H, Harashima H. Uptake pathways and subsequent intracellular trafficking in nonviral gene delivery. Pharmacol Rev 2006;58:32–45.
[28] Huang JG, Leshuka T, Gua FX. Emerging nanomaterials for targeting subcellular organelles. Nano Today 2011;6:478–92.
[29] Kiss AL, Botos E. Endocytosis via caveolae: alternative pathway with distinct cellular compartments to avoid lysosomal degradation? J Cell Mol Med 2009; 13:1228–37.
[30] Head BP, Patel HH, Roth DM, Murray F, Swaney JS, Niesman IR, et al. Microtubules and actin microfilaments regulate lipid raft/caveolae localization of adenylyl cyclase signaling components. J Biol Chem 2006;281:26391–9.
[31] Wong AW, Scales SJ, Reilly DE. DNA internalized via caveolae requires microtubule-dependent, Rab7-independent transport to the late endocytic pathway for delivery to the nucleus. J Biol Chem 2007;282:22953–63.
[32] Gratton SE, Ropp PA, Pohlhaus PD, Luft JC, Madden VJ, Napier ME, et al. The effect of particle design on cellular internalization pathways. Proc Natl Acad Sci U S A 2008;105:11613–8.